

# Establishment of patient-derived lung tumorspheres and their response to internal irradiation by Auger electrons

KARINA LINDBØG MADSEN<sup>1,2</sup>, NIELS LANGKJÆR<sup>1</sup>, OKE GERKE<sup>1,2</sup>,  
POUL F. HØILUND-CARLSEN<sup>1,2</sup> and BIRGITTE BRINKMANN OLSEN<sup>1,2</sup>

<sup>1</sup>Department of Nuclear Medicine, Odense University Hospital; <sup>2</sup>Department of Clinical Research, University of Southern Denmark, DK-5000 Odense C, Denmark

Received December 16, 2021; Accepted January 31, 2022

DOI: 10.3892/ijo.2022.5324

**Abstract.** The high recurrence rate of lung cancer is a major clinical challenge associated with therapy-resistant cancer stem cells (CSCs), which are rare subpopulations. Future successful treatment is required to also eradicate these subpopulations. Furthermore, the majority of anti-cancer treatments are being tested in adherent monolayer cultures with the limitations this entails in the translation of results into clinical practice. The present study aimed to establish and characterize patient-derived long-term primary lung cancer tumorspheres enriched in CSCs and evaluate the effects of Auger electrons on them. These electrons are emitted from radionuclides that decay by electron capture or internal conversion and have demonstrated promising therapeutic potential. Their low energy (<1 keV) is sufficiently potent to induce DNA double-strand breaks and eventually cell death while minimizing irradiation of non-targeted surrounding cells. Labeling a thymidine analog (deoxyuridine) with the Auger electron-emitting radionuclide [<sup>125</sup>I], which is exclusively incorporated into the DNA of proliferating cells during the S-phase, ensures a close distance to the DNA. Primary cell cultures grown as tumorspheres were established and characterized. The tumorspheres were morphologically distinct and differed concerning their proliferation rate and fraction of CSCs. Surface markers associated with CSCs were upregulated and 5-[<sup>125</sup>I]iodo-2'-deoxyuridine was incorporated in the tumorspheres. The Auger electrons induced DNA double-strand breaks, G2/M arrest and apoptosis in the tumorspheres; however, the tumorspheres derived from different patients exhibited heterogeneities in their sensitivity to Auger electron irradiation.

## Introduction

Lung cancer is the leading cause of cancer-related mortality in both genders and was responsible for 1.8 million deaths worldwide in 2020. The incidence of lung cancer is rising for females in North America and Northern Europe (1). Lung cancer is categorized into two types, namely non-small cell lung cancer (NSCLC), the predominant type that accounts for 85%, and SCLC (2). NSCLC has a five-year survival rate of ~20% (1), whereas SCLC has <5% due to aggressive behavior and early metastasis (3). NSCLC may be sub-classified into three groups based on histology: Squamous cell carcinoma, adenocarcinoma and large cell carcinoma (4). The treatment of lung cancer consists of surgery if detected early. Chemo- and radiotherapy and targeted therapy are the cornerstones for the treatment of SCLC and advanced NSCLC. However, a major drawback of current treatments is the development of resistance against chemo- and radiotherapy, as well as targeted therapies (5,6), a resistance that may be due to distinct subsets of cells within the tumor not being eliminated by conventional treatment. These subpopulations are the slow-proliferating cancer stem cells (CSCs). CSCs are characterized by self-renewal, differentiation potential, tumorigenic potential and high DNA repair capabilities (7). Challenges with CSCs are their ability to evade therapy and cells of this type display tumorigenic potential *in vivo* (8). To date, CSCs have been identified in various solid tumor types including, but not limited to, brain, breast, colorectal, prostate and lung cancer (9-13). CSCs are frequently identified based on their expression of surface markers and several markers have been proposed for lung cancer, including CD44, CD90, CD133, CD166 and epithelial cell adhesion molecule (EPCAM) [reviewed in (14)].

Auger electrons are emitted from radionuclides that decay by electron capture or internal conversion (15) and have demonstrated promising therapeutic potential in breast cancer, multiple myeloma and brain cancer (16-19). The low energy (<1 keV) of Auger electrons causes lethal damage to cancer cells when the emitter is close to the DNA (15). The electrons have a high linear energy transfer (~4-25 keV/μm) and travel within nanometers. Therefore, they are sufficiently potent to induce DNA double-strand breaks and eventually cell death, while minimizing irradiation of non-targeted surrounding cells (15,20). Labeling a thymidine analog with the Auger

---

*Correspondence to:* Dr Birgitte Brinkmann Olsen, Department of Nuclear Medicine, Odense University Hospital, Klørvænget 47, Entrance 44-46, DK-5000 Odense C, Denmark  
E-mail: birgitte.brinkmann.olsen@rsyd.dk

**Key words:** lung cancer, cancer stem cells, Auger electrons, thymidine analog, [<sup>125</sup>I]-UdR, DNA damage, cell cycle, apoptosis

electron-emitting radionuclide [<sup>125</sup>I], which is exclusively incorporated into the DNA of proliferating cells during the S-phase, ensures a close distance to the DNA (20).

Morgenroth *et al* (19) found that an Auger electron-emitting thymidine analog induced highly efficient death of CD133<sup>+</sup> glioblastoma stem cells (17) and multiple myeloma stem cells. In addition, Thisgaard *et al* (21) treated two immature glioblastoma spheroid cultures with 5-[<sup>125</sup>I]iodo-2'-deoxyuridine ([<sup>125</sup>I]I-UdR) and observed a dose-dependent reduction in cell survival. Furthermore, this inhibitory effect was also observed *in vivo* in orthotopically xenografted glioblastoma-bearing rats. Together, these results suggest that Auger electron emitters may overcome the resistance of CSCs. In the present study, the cellular responses to the thymidine analog [<sup>125</sup>I]I-UdR in patient-derived primary lung cancer cells grown as tumorspheres for CSC enrichment were evaluated.

## Materials and methods

**Establishment of primary cell cultures.** The primary cell cultures were established from resected NSCLC lung tumors collected at Odense University Hospital (Odense, Denmark) between February 2015 and July 2018. The inclusion criterion was surgery for primary lung cancer and exclusion criterion was prior radio- or chemotherapy. The Regional Ethics Committee of Southern Denmark approved the protocol (no. S-20140170). Tissue was washed twice with PBS containing 2% penicillin/streptomycin (Thermo Fisher Scientific, Inc.) and minced with scalpels. To prevent adherence, the tumorspheres were cultured in flasks coated with poly(2-hydroxyethyl methacrylate) (cat. no. P3932; MilliporeSigma). The cells were grown as tumorspheres in a serum-free medium at 37°C in a humidified incubator with 5% CO<sub>2</sub>. The serum-free medium consisted of DMEM/F-12 nutrient mix, Glutamax<sup>TM</sup> supplemented with 1% penicillin/streptomycin, 1% B27 (cat. no. 12587010), 20 ng/ml epidermal growth factor (cat. no. PHG0311; all from Thermo Fisher Scientific, Inc.) and 20 ng/ml basic fibroblast growth factor (cat. no. 100-18B; Peprotech, Inc.). Non-adherent conditions in serum-free medium were used to enrich CSCs and ensure homology to the parental tumor (22,23). Cells were expanded by mechanical dissociation or TrypLE<sup>TM</sup> Express (cat. no. 12605028; Thermo Fisher Scientific, Inc.) and used until 25 passages.

**Tumorsphere formation assay.** Cells (1 cell/well in 50 μl medium) were seeded in non-adherent 96-well plates (Deltalab). Wells containing only one cell were validated by microscopy and included in the experiment. Twice a week, 50 μl serum-free medium was added. After 21 days of incubation, the number of wells with one tumorsphere (>50 μm diameter) was determined microscopically (Leica DMIL LED; Leica Microsystems).

**Doubling time (DT).** Cells were seeded in non-adherent 24-well plates (Deltalab) at a density of 5x10<sup>4</sup> cells/well in 2 ml and counted every second day. The DT was calculated as  $DT = t(\log 2) / (\log N_t - \log N_0)$ , where *t* is the culture time and *N*<sub>0</sub> and *N*<sub>*t*</sub> are the initial and final cell numbers after seeding, respectively.

**Reverse transcription-quantitative PCR (RT-qPCR).** Total RNA was purified from adherent cells or tumorspheres using the RNeasy<sup>®</sup> Plus mini kit (cat. no. 74134; Qiagen GmbH) according to the manufacturer's protocol. The adherent cells were trypsinized tumorspheres that were allowed to grow in tissue culture-flasks in the presence of 10% fetal bovine serum to support their growth as differentiated cells. The RNA yield and quality were measured using the Qubit 4 Fluorometer (Thermo Fisher Scientific, Inc.) according to the manufacturer's protocols. RNA samples were stored at -80°C. RNA was reverse transcribed using the RevertAid Minus First-strand cDNA synthesis kit (cat. no. EP0451; Thermo Fisher Scientific, Inc.) using oligo(dT) primers (cat. no. SO131; Thermo Fisher Scientific, Inc.) according to the manufacturer's protocol, i.e., RNA was reverse transcribed at 42°C for 60 min and the reaction was terminated by heating to 70°C for 10 min. qPCR was performed with TaqMan Fast Advanced Master Mix (Thermo Fisher Scientific, Inc.) and Taqman assays for CD44 (Hs01075864\_m1), prominin 1 (PROM1; Hs01009250\_m1), Thy-1 cell surface antigen (also known as CD90; Hs00174816\_m1), SOX2 (Hs01053049\_s1), POU class 5 homeobox 1 (POU5F1; Hs0099632\_g1) and Nanog homeobox (NANOG; Hs04260366\_g1) (Thermo Fisher Scientific, Inc.). A total of 20 ng cDNA was used per reaction and the qPCR cycling was performed on a QuantStudio 3 (Applied Biosystems; Thermo Fisher Scientific, Inc.) as follows: 50°C for 2 min and 95°C for 2 min, and then 40 cycles of 95°C for 1 sec and 60°C for 20 sec. All reactions were performed in triplicate and normalized to hypoxanthine phosphoribosyltransferase 1 (HPRT1; Hs02800695\_m1). Initially, five candidate reference genes (HPRT1, RPLP0, B2M, GAPDH and ACTB) were tested and HPRT1 was the most stable in the experiments when using the web-based analysis tool RefFinder (24). Relative quantification was performed using the  $\Delta\Delta C_q$  method (25).

**Proliferation.** Cells were seeded in non-adherent 24-well plates (1x10<sup>5</sup>) and incubated with 10 μM 5-ethynyl-2'-deoxyuridine (EdU) (cat. no. BCK-EDU488; MilliporeSigma) for 24 h. Subsequently, the cells were fixed with 3.7% formaldehyde (cat. no. 47608; MilliporeSigma) for 15 min at room temperature and permeabilized in 0.5% Triton X-100 (cat. no. T8787; MilliporeSigma) in PBS for 20 min at room temperature. The cells were stained using the Click-iT EdU 488 Proliferation Kit (cat. no. BCK-EDU488; MilliporeSigma) following the manufacturer's protocol and counterstained with 10 μg/ml DAPI (cat. no. D8417; MilliporeSigma) for 10 min. For each group, 300 cells were analyzed by fluorescent microscopy using a Leica DM 2000 LED microscope (Leica Microsystems). Quantification of EdU-positive and -negative cells was performed manually using the 'cell counter plugin' in ImageJ version 1.50i (National Institutes of Health).

**Cellular uptake and DNA incorporation of [<sup>125</sup>I]I-UdR.** For each experimental condition, 100,000 cells were incubated with 18.5 kBq/ml [<sup>125</sup>I]I-UdR [prepared as in (26)] in 1 ml serum-free medium for 1, 4 and 7 h in non-adherent 24-well plates. At each time-point, the experiment was ended by washing cells twice with 400 μl cold PBS and twice with 400 μl 5% trichloroacetic acid (TCA). The DNA was solubilized in 500 μl 1M NaOH. The radioactivity in the TCA

fractions and collected DNA was determined in a 2470 Wizard Automatic Gamma Counter (Perkin Elmer). Cellular uptake was calculated as the sum of the radioactivity in the TCA fractions and collected DNA relative to the added radioactivity (% of injected dose/well). DNA incorporation was calculated as the percentage of radioactivity in the DNA relative to the cellular uptake.

**Viability assay.** A total of 1,000 single cells were seeded in quadruplicate in non-adherent 96-well plates in 50  $\mu$ l serum-free medium with 0.1-6.0 kBq/ml [<sup>125</sup>I]I-UdR in 50  $\mu$ l medium. As a control, the non-radioactive, but chemically identical [<sup>127</sup>I]I-UdR (24 pg/ml; cat. no. I7125; MilliporeSigma) corresponding to the mass concentration of 6 kBq/ml was also tested. On day seven, the cell viability was evaluated by adding 13  $\mu$ l CellTiter-Blue (cat. no. G8080; Promega Corporation) to each well. Fluorescence was measured at 520 nm excitation/580-640 nm emission in a GloMax Explorer (Promega Corporation).

**Clonogenic assay.** A total of 100 cells were seeded in non-adherent 24-well plates in 1 ml medium and incubated with 2.5 or 5 kBq/ml [<sup>125</sup>I]I-UdR. The number of tumorspheres was evaluated after 10 [lung cancer case no. 10 (LUC10) and LUC13] or 17 days (LUC6) using a Leica DM IL LED microscope (Leica Microsystems).

**Cell cycle analysis.** A total of 100,000 cells were incubated with 2.5 kBq/ml [<sup>125</sup>I]I-UdR for seven days. The LUC6 tumorspheres were mechanically dissociated by pipetting, and LUC10 and LUC13 were trypsinized, washed once with PBS and fixed in 70% ethanol at -20°C overnight. After fixation, cells were washed once in PBS and resuspended in 100  $\mu$ l cell cycle reagent mix [20  $\mu$ g/ml propidium iodide (cat. no. P4170) and 10 mg/ml RNase A (cat. no. 10109142001); both from MilliporeSigma] and incubated in the dark at room temperature for 30 min. Next, cells were washed in 100  $\mu$ l PBS and loaded into an A8 cassette (Chemometec). The cell cycle distribution was measured by image cytometry in the Nucleocounter NC-3000 (Chemometec).

**Apoptosis and DNA damage.** A total of 100,000 cells were incubated with 2.5 kBq/ml [<sup>125</sup>I]I-UdR for seven days, dissociated and counted using the MUSE Count and Viability reagent (cat. no. 4000-0335; Luminex). Cells were resuspended in 50  $\mu$ l 1% bovine serum albumin (cat. no. A8022)/PBS for the apoptosis analysis and mixed with 50  $\mu$ l MUSE Annexin V and Dead reagent (cat. no. 4700-1485; Luminex). The samples were incubated at room temperature in the dark for 20 min prior to analysis of 10,000 cells on the Guava MUSE Cell Analyzer (Luminex).

DNA damage was analyzed using the MUSE H2AX Activation Kit (cat. no. MCH200101; Luminex). In brief, dissociated cells were resuspended in 50  $\mu$ l 1X Assay buffer and 50  $\mu$ l fixation reagent for 5 min on ice. Subsequently, the cells were permeabilized in 50  $\mu$ l ice-cold permeabilization reagent for 5 min on ice. Cells were incubated in 50  $\mu$ l 1X Assay buffer containing 1  $\mu$ l anti-H2A.X (cat. no. CS208162; Luminex) and 1  $\mu$ l anti-phosphorylated-histone H2A.X (phospho-H2A.X; cat. no. CS208174; Luminex) at room temperature in the dark for 30 min. Cells were washed with 100  $\mu$ l 1X Assay buffer

and resuspended in 200  $\mu$ l 1X Assay buffer, and 1,000 cells were analyzed on the Guava MUSE Cell Analyzer (Luminex).

**Statistical analysis.** Experiments were performed as three independent replicates and descriptive statistics for quantitative measurements comprised the mean  $\pm$  standard error of the mean. One-way ANOVA was used to compare means of sphere-formation, means of EdU/DAPI-positive cells and means of cellular uptake and incorporation (correction for multiple comparisons: Tukey). Cellular uptake and incorporation were also evaluated by a post-test for a linear trend. Differences between means in viability and the effect of [<sup>125</sup>I]I-UdR on tumorsphere growth were evaluated by one-way ANOVA (correction for multiple comparisons: Dunnett/Bonferroni). Two-way ANOVA was applied to compare the means from the cell cycle analysis (cell cycle phase and treatment as independent factors; correction for multiple comparisons: Šidák) and RT-qPCR analysis (gene and sample as independent factors; correction for multiple comparisons: Tukey). Differences between the mean values for cell death and DNA damage were investigated by an unpaired t-test. P<0.05 was considered as a threshold of statistical significance. Statistical tests were performed using GraphPad Prism version 9.0 (GraphPad Software, Inc.).

## Results

**Patient characteristics.** Tissue was collected from 15 patients whose details are provided in Table I. The median patient age was 70 years (range, 57-85 years) and 60% were males. No vital tumorspheres were formed in four of them, which were therefore discarded. The remaining samples initially gave rise to viable tumorspheres, but some samples were not susceptible to long-term culture. In the end, only LUC6, LUC10 and LUC13 exhibited stable unlimited exponential growth even in later passages.

**Tumorsphere morphology, tumorsphere formation and population DT.** LUC6, LUC10 and LUC13 all demonstrated the ability to form vital tumorspheres (Fig. 1A), one of the hallmarks of CSCs (27). LUC6 tumorspheres were loosely packed with an irregular surface and clearly defined cells. The LUC10 tumorspheres were encapsulated with a membrane-like structure and densely packed cells, whereas spheroid cells were more defined and the tumorsphere-surface appeared more irregular in LUC13. CSCs are also defined by their ability to self-renew, which is a functional difference from non-CSCs (7). Self-renewal may be assessed by the sphere formation assay, which only considers tumorspheres formed from one single cell. The results indicated that LUC10 (P<0.05) and LUC13 contained more cells with self-renewing potential than LUC6 (Fig. 1B). The population DT was estimated for the tumorspheres (Fig. 1C): The DT of LUC6 was 1.5 $\pm$ 0.11 days. LUC10 and LUC13 had population DTs of 2.8 $\pm$ 0.06 and 3.4 $\pm$ 0.11 days, respectively. The relative expression levels of the stemness-related surface markers CD44, THY1 (CD90), PROM1 (CD133), SOX2, NANOG and POU5F1 (Oct4) in LUC10 and LUC13 tumorspheres compared to adherent cells were also evaluated (Fig. 1D and E). LUC10 cells grown as tumorspheres exhibited significantly increased

Table I. Characteristics of patients and tumorsphere formation ability of their samples.

Patient code	Sex	Age (years)	Tumorsphere formation	Histology
LUC1	Female	57	+/-	Planocellular carcinoma
LUC2	Male	70	+/-	Mucinous adenocarcinoma
LUC3	Female	77	+/-	Adenocarcinoma
LUC4	Female	77	-	Planocellular carcinoma
LUC5	Male	70	-	Adenocarcinoma
LUC6	Male	62	+	Adenocarcinoma
LUC7	Male	68	+/-	Papillary adenocarcinoma
LUC8	Male	70	+/-	Planocellular carcinoma
LUC9	Female	85	-	Planocellular carcinoma
LUC10	Female	66	+	Adenosquamous carcinoma
LUC11	Male	76	-	Adenocarcinoma
LUC12	Male	67	+/-	Adenocarcinoma
LUC13	Male	67	+	Pleomorphic carcinoma
LUC14	Female	75	+/-	Adenocarcinoma
LUC15	Male	74	+/-	Planocellular carcinoma

(-), No vital tumorspheres; (+/-), only short-term culture; (+) long-term culture; LUC, lung cancer case.

expression THY1 ( $P<0.01$ ) and SOX2 ( $P<0.05$ ) compared to adherent LUC10 cells (Fig. 1D). Likewise, LUC13 tumorspheres displayed significantly increased expression of CD44 ( $P<0.0001$ ), SOX2 ( $P<0.0001$ ) and NANOG ( $P<0.01$ ) compared to adherent cells (Fig. 1E). Adherently grown LUC10 and LUC13 expressed higher levels of PROM1; however, the difference was not significant. Unfortunately, it was not possible to grow adherent LUC6 cells, so instead, the expression of LUC6 tumorspheres was compared to LUC10 and LUC13 tumorspheres (Fig. 1F and G). LUC6 expressed significantly lower levels of CD44 and PROM1 than LUC10 ( $P<0.05$ ) and significantly lower levels of CD44 ( $P<0.0001$ ) than LUC13. These results support the notion that LUC10 and LUC13 contained more CSCs than LUC6.

**Proliferation.** The thymidine analog EdU was used to determine the proportion of proliferating cells in the tumorspheres (Fig. 2A). Most of the LUC6 cells in the tumorspheres were EdU-positive ( $98.6\pm 1.3\%$ ). Approximately half ( $48.3\pm 9.7\%$ ) of the LUC13 cells were proliferative, whereas EdU-positive LUC10 cells accounted for  $63.6\pm 12.4\%$  in the tumorspheres (Fig. 2B). Incorporation of EdU was present in all three samples within 24 h, and correlated with the DT.

**$[^{125}\text{I}]\text{-UdR}$  uptake and incorporation.** Cellular uptake and DNA incorporation of  $[^{125}\text{I}]\text{-UdR}$  were measured after 1, 4 and 7 h (Fig. 3). These time-points were chosen to minimize cytotoxicity resulting from long exposure times (28). In addition, it was previously reported that DNA incorporation was rapid within the first 4-5 h and plateaued by 10 h (29). Overall, the cellular uptake of  $[^{125}\text{I}]\text{-UdR}$  in LUC6 and LUC10 increased significantly over time (post-test for linear trend,  $P<0.0001$ ). A significantly increased cellular uptake was also seen for LUC13 between 1 and 7 h ( $P<0.05$ ), although  $[^{125}\text{I}]\text{-UdR}$  uptake was not doubled (post-test for linear trend,  $P<0.05$ ) (Fig. 3A).

$[^{125}\text{I}]\text{-UdR}$  incorporation in LUC6 and LUC10 increased significantly ( $P<0.0001$ ) from  $\sim 28$  to 79 and 88%, respectively (post-test for linear trend between the time-points,  $P<0.0001$ ) (Fig. 3B). The DNA incorporation in LUC13 increased significantly from 1 h, where 16%  $[^{125}\text{I}]\text{-UdR}$  was incorporated, to 52 and 70% after 4 and 7 h, respectively ( $P<0.0001$ ). Furthermore, the difference in the incorporation of  $[^{125}\text{I}]\text{-UdR}$  from 4 to 7 h was also significant ( $P<0.001$ ; post-test for linear trend,  $P<0.0001$ ). Overall, DNA incorporation of  $[^{125}\text{I}]\text{-UdR}$  increased over time; however, the level varied among the different tumorspheres.

**Viability.** Next, the effect of  $[^{125}\text{I}]\text{-UdR}$  on the viability of the tumorspheres was assessed by incubating with 0.1-6 kBq/ml  $[^{125}\text{I}]\text{-UdR}$  for seven days, followed by CellTiter-Blue viability measurements (Fig. 4). The viability of LUC6 significantly decreased at all activities tested ( $P<0.0001$ ) compared to 0 kBq/ml  $[^{125}\text{I}]\text{-UdR}$ . The viability was  $\sim 50\%$  when LUC6 was treated with 0.25 kBq/ml  $[^{125}\text{I}]\text{-UdR}$ . The viability of LUC6 did not decrease further when the activity exceeded 2 kBq/ml. The viability of LUC10 also significantly decreased at all tested activities of  $[^{125}\text{I}]\text{-UdR}$  ( $P<0.0001$ ; and 0.1 kBq/ml,  $P<0.001$ ). LUC13 was more resistant to  $[^{125}\text{I}]\text{-UdR}$ , as 3 kBq/ml was necessary to reduce the viability to  $\sim 50\%$ . Furthermore, the viability of LUC13 was still  $>30\%$  when treated with 6 kBq/ml. The non-radioactive and chemically identical  $[^{127}\text{I}]\text{-UdR}$  did not decrease the viability (results not shown). Overall, there was an activity concentration-dependent decrease in viability; however, LUC6 was more sensitive to  $[^{125}\text{I}]\text{-UdR}$  than LUC10 and LUC13.

**Effect of  $[^{125}\text{I}]\text{-UdR}$  on clonogenic survival.** The effect of  $[^{125}\text{I}]\text{-UdR}$  on tumorsphere formation was then investigated by incubating 100 cells with 0, 2.5 and 5 kBq/ml  $[^{125}\text{I}]\text{-UdR}$  (Fig. 5). Tumorspheres were counted following 10 (LUC10

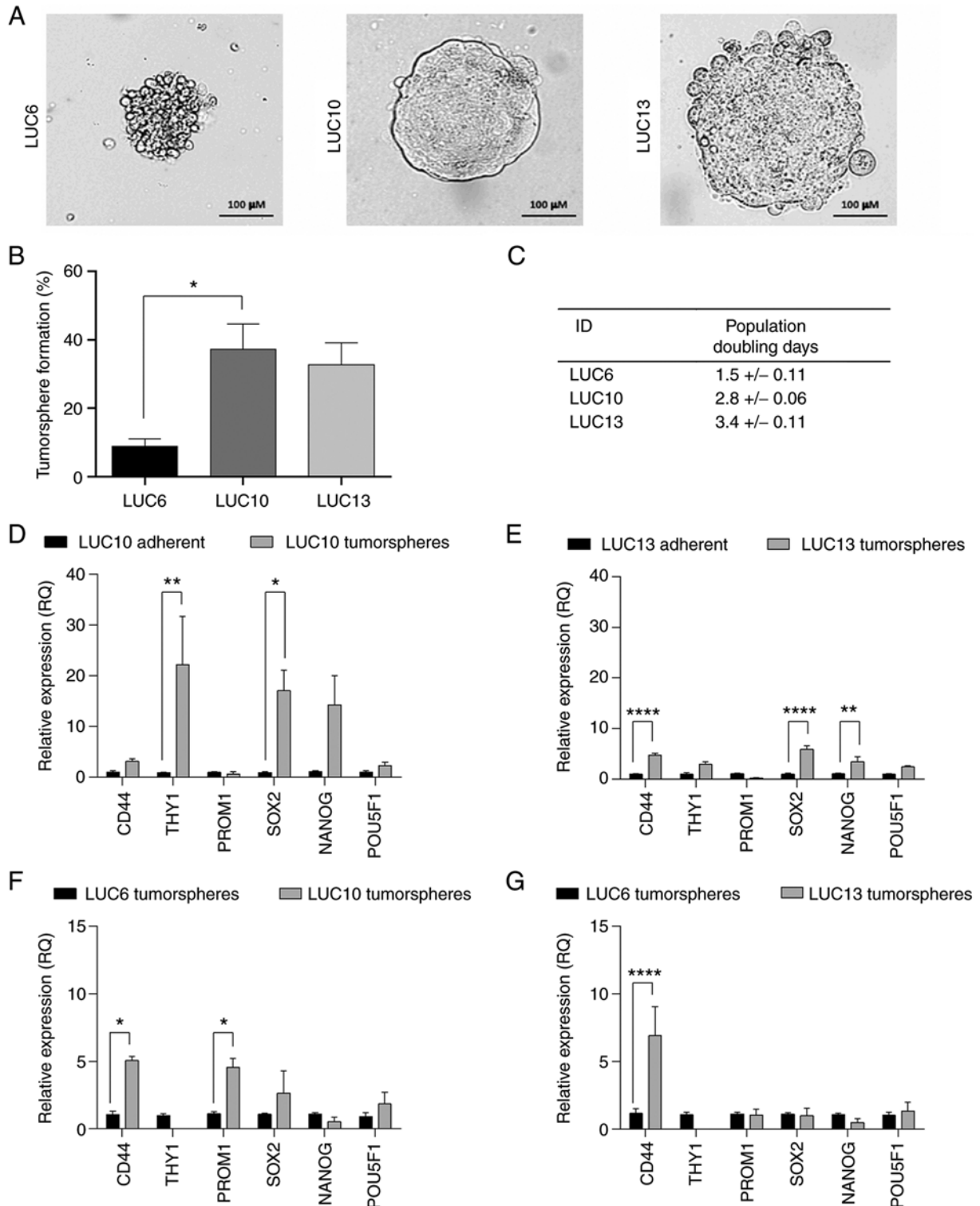


Figure 1. Morphology and tumorsphere formation. (A) Representative images of LUC6, LUC10 and LUC13 tumorspheres (scale bar, 100  $\mu$ m). (B) Evaluation of the ability to generate tumorspheres from a single cell. (C) Estimation of population doubling time for cells grown as tumorspheres. (D) Relative expression of cancer stem cell-related markers in adherent LUC10 cells and LUC10 tumorspheres. (E) Relative expression of cancer stem cell-related markers in adherent LUC13 cells and LUC13 tumorspheres. (F) Relative expression of cancer stem cell-related markers in LUC6 and LUC10 tumorspheres. (G) Relative expression of cancer stem cell-related markers in LUC6 and LUC13 tumorspheres. Expression results were normalized to hypoxanthine phosphoribosyltransferase 1. Experiments were performed as three independent replicates. Values are expressed as the mean  $\pm$  standard error of the mean. \* $P < 0.05$ , \*\* $P < 0.01$  and \*\*\*\* $P < 0.0001$ . RQ, relative quantification; LUC6, lung cancer case no. 6; THY1, Thy-1 cell surface antigen; PROM1, prominin 1; NANOG, Nanog homeobox; POU5F1, POU class 5 homeobox 1.

and LUC13) or 17 days (LUC6) after the addition of [ $^{125}$ I] I-UdR. The number of tumorspheres generated from [ $^{125}$ I] I-UdR-treated cells was normalized to that of tumorspheres

generated from untreated control cells. Treatment of LUC6 with 2.5 kBq/ml led to a significant decrease in the number of tumorspheres to  $32.5 \pm 8.8\%$  ( $P < 0.01$ ). Treatment with

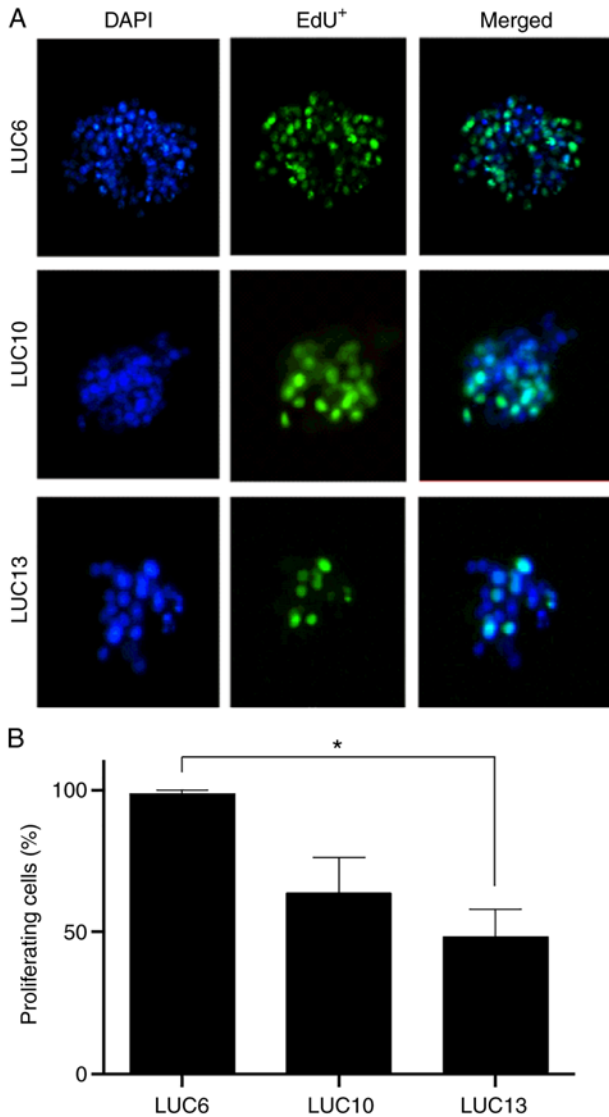


Figure 2. Proliferation assay. (A) Representative fluorescence microscopy images of tumorspheres labeled with EdU and counterstained with DAPI (magnification, x20). (B) Quantification of EdU/DAPI-positive cells (proliferating cells). Experiments were performed as three independent replicates. Values are expressed as the mean  $\pm$  standard error of the mean. \* $P < 0.05$ . EdU, 5-ethynyl-2'-deoxyuridine; LUC6, lung cancer case no. 6.

5 kBq/ml further reduced the formation of LUC6 tumorspheres significantly to  $11.3 \pm 2.1\%$  ( $P < 0.001$ ). The number of LUC10 tumorspheres decreased to  $44.6 \pm 14.9$  and  $44.6 \pm 18.6\%$  when treated with 2.5 and 5 kBq/ml [ $^{125}\text{I}$ ]I-UdR, respectively, yet not significantly. Treatment with 2.5 kBq/ml decreased the number of LUC13 tumorspheres significantly to  $50.8 \pm 6.2\%$  ( $P < 0.05$ ) and following treatment with 5 kBq/ml, only  $29.3 \pm 10.3\%$  tumorspheres were formed ( $P < 0.01$ ). Overall, [ $^{125}\text{I}$ ]I-UdR decreased the ability of LUC6 and LUC13 to form tumorspheres in a concentration-dependent manner. By contrast, the ability of LUC10 to form tumorspheres did not further decrease when treated with 5 kBq/ml compared to 2.5 kBq/ml [ $^{125}\text{I}$ ]I-UdR.

**Radiation-induced DNA damage.** The DNA-damaging effect of 2.5 kBq/ml [ $^{125}\text{I}$ ]I-UdR was investigated by analyzing the phosphorylation of H2AX as a marker of DNA double-strand

breaks (Fig. 6A) (30). The level of phospho-H2AX in LUC6 increased from  $7.2 \pm 0.3$  to  $14.8 \pm 2.2\%$  upon [ $^{125}\text{I}$ ]I-UdR treatment ( $P < 0.05$ ). Exposure to [ $^{125}\text{I}$ ]I-UdR significantly increased the percentage of phospho-H2AX in LUC10 from  $3.9 \pm 0.6$  to  $11.1 \pm 0.8\%$  ( $P < 0.01$ ). Likewise, the increase of phospho-H2AX from  $3.6 \pm 0.2$  to  $11.8 \pm 0.8\%$  in LUC13 was significant ( $P < 0.001$ ). [ $^{125}\text{I}$ ]I-UdR induced phospho-H2AX activation at varying percentages; the most significant increase in phospho-H2AX was observed in LUC10 and LUC13 (Fig. 6B).

**Cell cycle.** Auger electrons are sufficiently potent to induce DNA double-strand breaks and thereby cell-cycle arrest; thus, the cell cycle distribution of control cells and cells treated with 2.5 kBq/ml [ $^{125}\text{I}$ ]I-UdR for seven days was analyzed (Fig. 7A). [ $^{125}\text{I}$ ]I-UdR significantly increased the percentage of LUC6 in subG1 phase from  $3.9 \pm 0.3$  to  $12.2 \pm 1.2\%$  ( $P < 0.01$ ) and that in G2/M phase from  $16.9 \pm 1.4$  to  $30.9 \pm 1.6\%$  ( $P < 0.001$ ). Furthermore, the percentage of LUC6 in G0/G1 phase decreased significantly from  $71.3 \pm 0.6$  to  $47.5 \pm 1.6\%$  ( $P < 0.0001$ ) upon [ $^{125}\text{I}$ ]I-UdR treatment. The proportion of LUC10 in G0/G1 significantly decreased from  $78.6 \pm 1.8$  to  $70.1 \pm 1.4\%$  in response to [ $^{125}\text{I}$ ]I-UdR ( $P < 0.0001$ ). Furthermore, [ $^{125}\text{I}$ ]I-UdR significantly increased LUC10 in G2/M-phase from  $10.3 \pm 1.1$  to  $15.8 \pm 1.0\%$  ( $P < 0.01$ ), but unlike for LUC6, there were only minor increases in the proportion of LUC10 in subG1 phase. The proportion of LUC13 in G0/G1 phase significantly decreased from  $83.6 \pm 0.4$  to  $72.3 \pm 0.6\%$  when treated with [ $^{125}\text{I}$ ]I-UdR ( $P < 0.0001$ ) and G2/M significantly increased from  $9.0 \pm 0.2$  to  $17.8 \pm 0.4\%$  ( $P < 0.001$ ) as well as cells in S ( $P < 0.05$ ; Fig. 7B). Overall, [ $^{125}\text{I}$ ]I-UdR increased the subG1 and G2/M phase populations and decreased the percentage of cells in G0/G1 phase.

**Radiation-induced apoptosis.** Radiation-induced DNA damage may lead to apoptosis if it remains unrepaired (31). In the present study, Annexin V-positive cells (apoptotic) were evaluated following treatment with 2.5 kBq/ml [ $^{125}\text{I}$ ]I-UdR for 7 days (Fig. 8). [ $^{125}\text{I}$ ]I-UdR increased Annexin V-positive LUC6, LUC10, and LUC13 significantly by  $2.65 \pm 0.16$ - ( $P < 0.001$ ),  $2.38 \pm 0.23$ - ( $P < 0.01$ ) and  $1.85 \pm 0.16$ - ( $P < 0.01$ ) fold, respectively. Apoptosis was highest in LUC6, corresponding to the results of the cell cycle analysis, where a significant increase in subG1 was observed in LUC6.

## Discussion

The high recurrence rate of lung cancer is a major clinical challenge and is associated with therapy-resistant CSCs (7,8). The vast majority of anti-cancer treatments are tested preclinically *in vitro* in adherent monolayer cells, which may lead to insufficient efficacy in cancer patients (32). In the present study, patient-derived NSCLC tumorspheres were established and characterized and the effects of the Auger electron-emitting compound [ $^{125}\text{I}$ ]I-UdR, which previously proved effective against CSCs from glioblastoma and multiple myeloma (17,19,21,26), were evaluated. The tumorspheres were morphologically distinct and differed concerning their proliferation rate and doubling time. However, this was not correlated with their ability to form tumorspheres. Surface markers associated with CSCs were upregulated in the tumorspheres

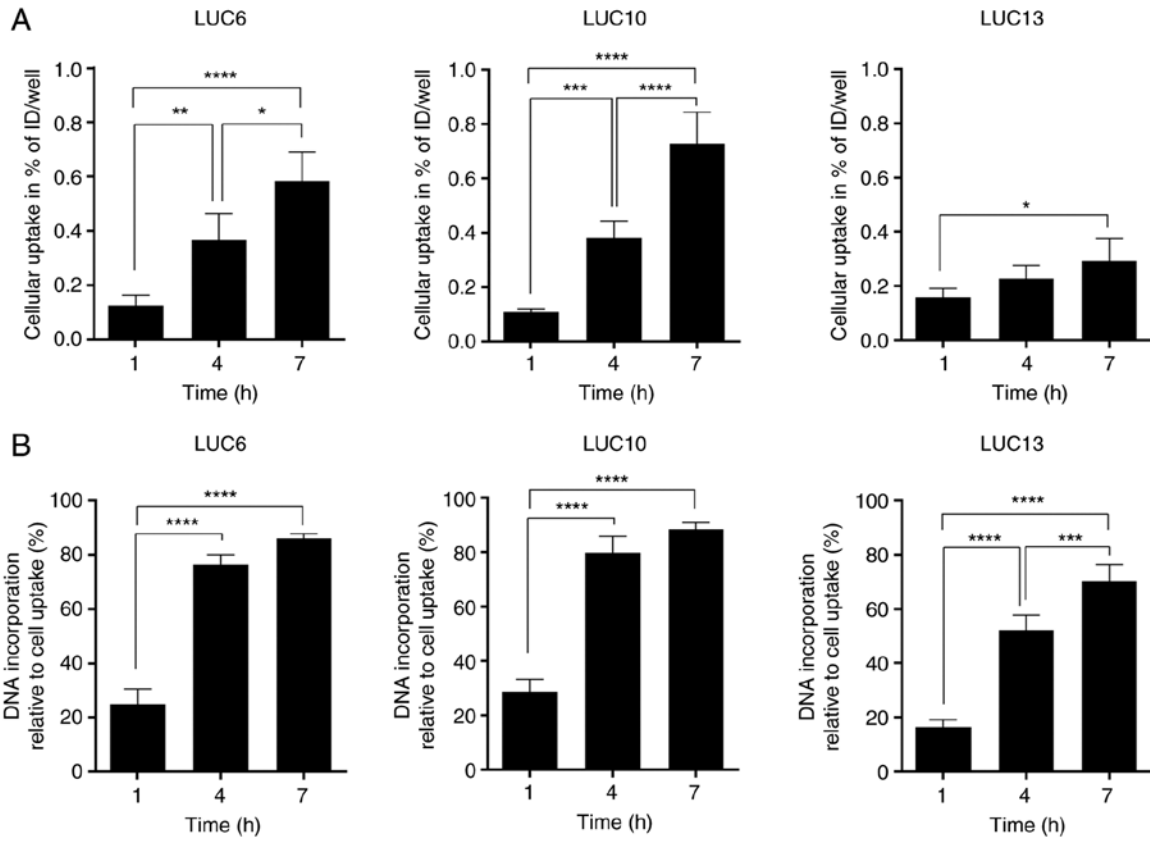


Figure 3. Cellular uptake and DNA incorporation of [ $^{125}\text{I}$ ]I-UdR. (A) Cellular uptake of 18.5 kBq/ml [ $^{125}\text{I}$ ]I-UdR in LUC6, LUC10 and LUC13 after 1, 4 and 7 h of incubation. (B) DNA incorporation of [ $^{125}\text{I}$ ]I-UdR relative to cell uptake. Experiments were performed in duplicates and independently repeated three times. Values are expressed as the mean  $\pm$  standard error of the mean. \* $P < 0.05$ , \*\* $P < 0.01$ , \*\*\* $P < 0.001$  and \*\*\*\* $P < 0.0001$ . LUC6, lung cancer case no. 6; [ $^{125}\text{I}$ ]I-UdR, 5- $^{125}\text{I}$ iodo-2'-deoxyuridine; ID, injected dose.

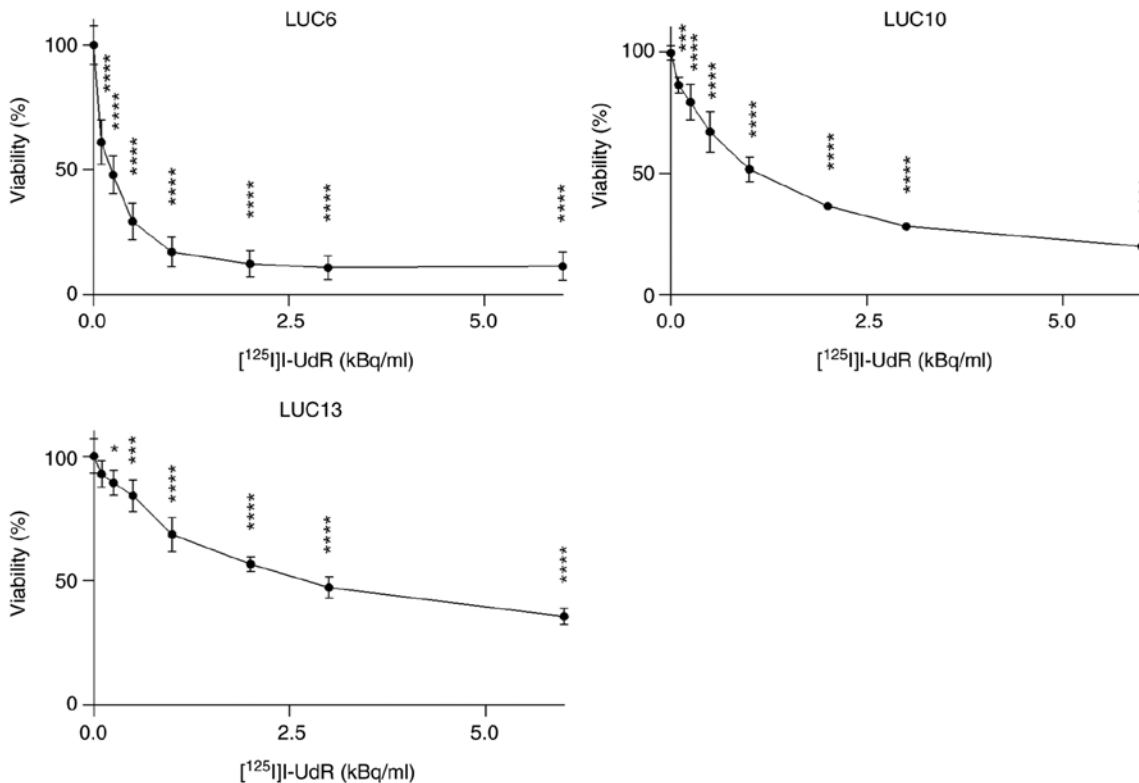


Figure 4. Cell viability after incubation with [ $^{125}\text{I}$ ]I-UdR for 7 days. The viability was evaluated using the CellTiter-Blue assay and results were normalized to control cells. Experiments were performed in quadruplicates and repeated three times independently. Values are expressed as the mean  $\pm$  standard error of the mean. \* $P < 0.05$ , \*\* $P < 0.01$  and \*\*\*\* $P < 0.0001$  compared to the control. [ $^{125}\text{I}$ ]I-UdR, 5- $^{125}\text{I}$ iodo-2'-deoxyuridine; LUC6, lung cancer case no. 6.

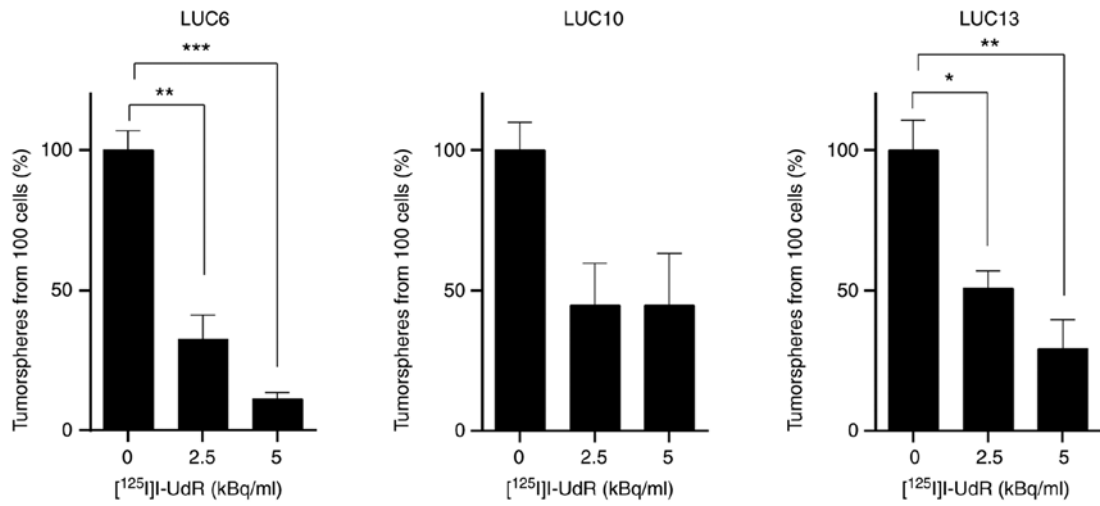


Figure 5. Effect of [ $^{125}\text{I}$ ]-UdR on tumorsphere formation. The number of tumorspheres from 100 single cells after treatment with 0, 2.5 or 5 kBq/ml [ $^{125}\text{I}$ ]-UdR normalized to the untreated control cells. Experiments were performed as three independent replicates. Values are expressed as the mean  $\pm$  standard error of the mean. \* $P < 0.05$ , \*\* $P < 0.01$  and \*\*\* $P < 0.001$ . [ $^{125}\text{I}$ ]-UdR, 5-[ $^{125}\text{I}$ ]iodo-2'-deoxyuridine; LUC6, lung cancer case no. 6.

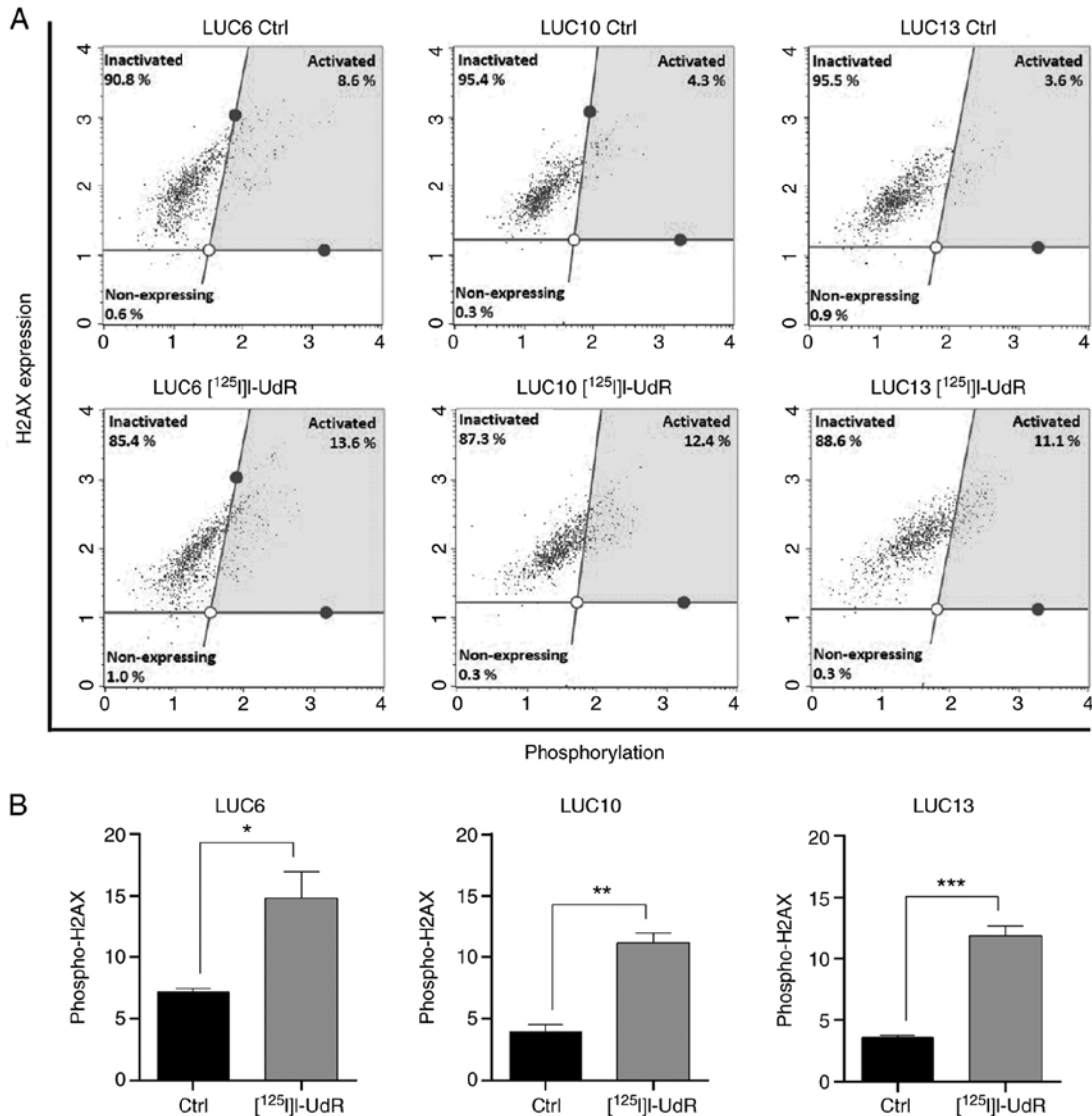


Figure 6. Radiation-induced DNA damage. (A) Representative dot-plots of DNA double-strand breaks identified by detecting phospho-H2AX. (B) Percentage of phospho-H2AX-positive cells after treatment with 2.5 kBq/ml [ $^{125}\text{I}$ ]-UdR for 7 days compared to untreated control cells. Experiments were performed as three independent replicates. Values are expressed as the mean  $\pm$  standard error of the mean. \* $P < 0.05$ , \*\* $P < 0.01$  and \*\*\* $P < 0.001$ . [ $^{125}\text{I}$ ]-UdR, 5-[ $^{125}\text{I}$ ]iodo-2'-deoxyuridine; LUC6, lung cancer case no. 6; Ctrl, control; phospho-H2AX, phosphorylated H2AX.

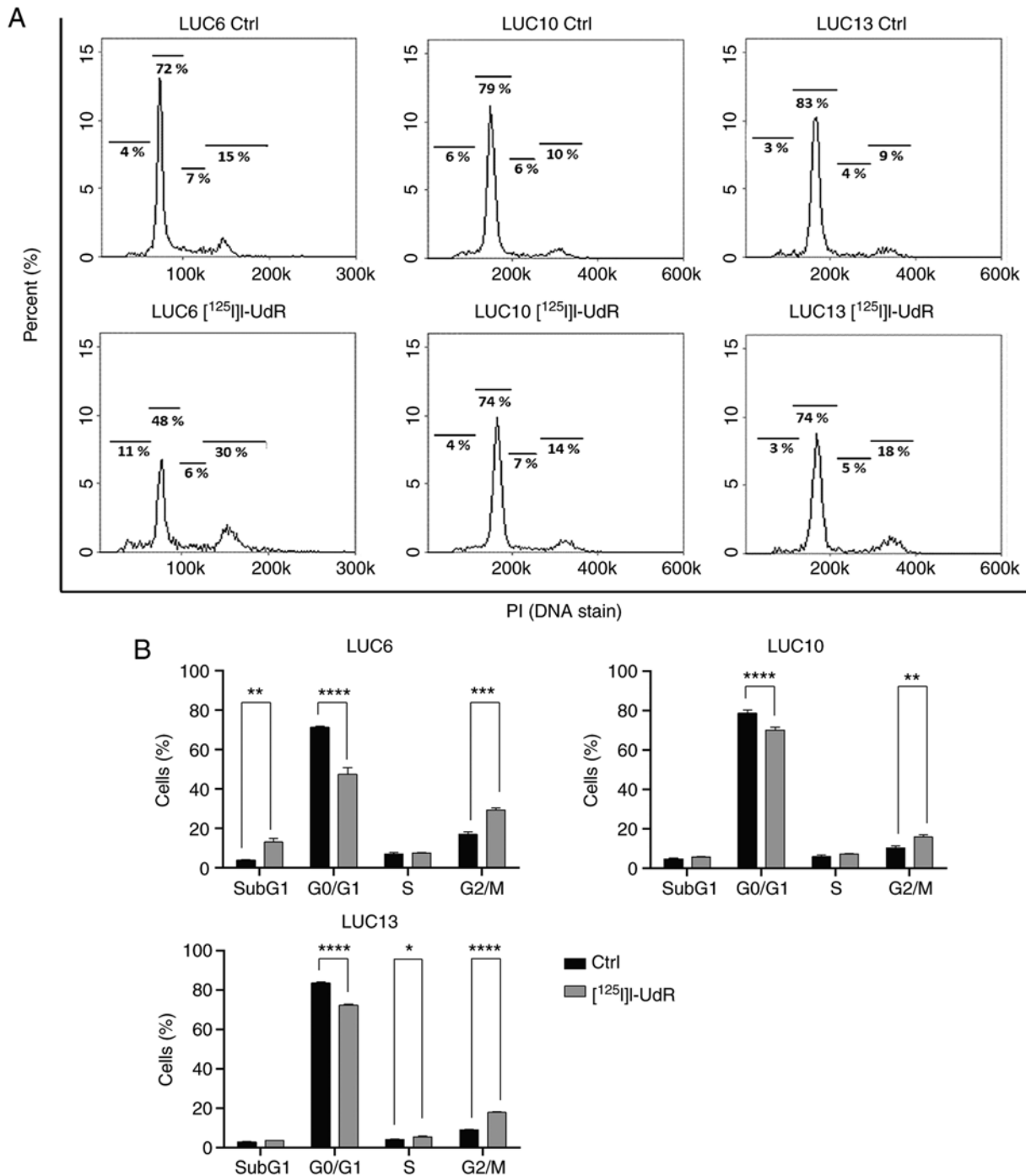


Figure 7. Cell cycle analysis. (A) Representative cell cycle histograms of untreated control and after treatment with 2.5 kBq/ml [<sup>125</sup>I]-UdR for 7 days. (B) Quantitative analysis. Experiments were performed as three independent replicates. Values are expressed as the mean  $\pm$  standard error of the mean. \*P<0.05, \*\*P<0.01, \*\*\*P<0.001 and \*\*\*\*P<0.0001. [<sup>125</sup>I]-UdR, 5-[<sup>125</sup>I]iodo-2'-deoxyuridine; LUC6, lung cancer case no. 6; Ctrl, control.

compared to those in adherent cells. Incorporation of [<sup>125</sup>I]-UdR led to DNA double-strand breaks, G2/M arrest and apoptosis, while samples from different patients exhibited various degrees of sensitivity to Auger electron irradiation.

Tumorspheres are non-adherent three-dimensional cell cultures grown in serum-free medium. The technique is based on self-renewal and anoikis resistance (22,32,33). It enriches for cells with stemness features, including self-renewal, unlimited growth abilities, tumorigenic potential *in vivo*, ability to differentiate, high invasion capacity and resistance to high doses of chemotherapy (22,33). Tumorspheres are also

more representative of the parental tumor than cells grown in two-dimensional systems (22,23). Furthermore, they are independent of surface markers, which thus eliminates the use for unique markers whose identification in lung CSCs remains challenging (34,35).

However, establishing primary stable long-term tumorspheres may be challenging and the success rate in the present study was only 20%. This is lower than the 35-40% previously obtained for lung cancer (22,33), which may be due to experimental design variables, such as the tumor stage and genetics (36,37). Certain cultures were only able to expand

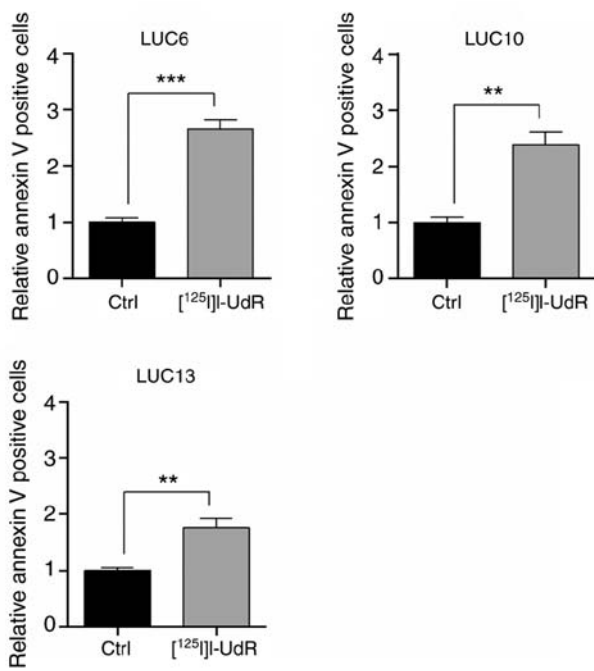


Figure 8. Radiation-induced apoptosis (Annexin V-positive cells). Apoptosis after treatment with 2.5 kBq/ml [<sup>125</sup>I]I-UdR for 7 days normalized to untreated control. Experiments were performed as three independent replicates. Values are expressed as the mean ± standard error of the mean. \*\*P<0.01 and \*\*\*P<0.001. [<sup>125</sup>I]I-UdR, 5-[<sup>125</sup>I]iodo-2'-deoxyuridine; LUC6, lung cancer case no. 6; Ctrl, control.

short-term, suggesting that the tumorspheres depended on factors not provided by the medium (37). Certain tumorspheres were not sufficiently stable for propagation and may have represented aggregates rather than true tumorspheres (38).

Overall, it was observed that LUC10 and LUC13 contained more CSCs than LUC6. This was supported by a tumorsphere formation efficiency assay (i.e., one single cell/well) to determine the frequency of CSCs in the population, where a higher frequency in LUC10 and LUC13 was observed. CSCs are considered slow-proliferating (36,39) and in the present study, it was also observed that almost all of the LUC6 cells incorporated the thymidine analog EdU, whereas the incorporation was lower in LUC10 and LUC13. These results were also supported by the analysis of DTs, where it was determined that LUC6 had the shortest DT, again supporting that LUC10 and LUC13 contain a higher frequency of CSCs than LUC6. Furthermore, the RT-qPCR analysis indicated that LUC6 tumorspheres expressed lower levels of CSC-related genes than LUC10 and LUC13 tumorspheres.

When the expression of selected CSC-genes in LUC10 and LUC13 tumorspheres was compared with that in their adherent counterparts, it was observed that the surface markers CD44 and THY1 (CD90) and the stemness transcription factors NANOG and SOX2 were upregulated. Unexpectedly, PROM1 (CD133) and POU5F1 (Oct4) were not significantly upregulated in the tumorspheres. Eramo *et al* (33) previously identified a CD133<sup>+</sup> subpopulation in lung cancer that was able to form tumorspheres and was tumorigenic in mice. By contrast, Herreros-Pomares *et al* (22) were not able to detect any PROM1 transcripts in eight patient-derived tumorspheres and they did not observe that POU5F1 (Oct4) was significantly

upregulated in tumorspheres. Furthermore, Park *et al* (40) obtained differences among NSCLC subtypes, e.g., there was no detectable protein expression of CD133 and Oct4 in squamous cell carcinoma.

All three tumorsphere cultures incorporated [<sup>125</sup>I]I-UdR; the lowest uptake was, as expected, observed in the slower proliferating LUC13 spheres. The uptake and incorporation of thymidine analogs in cancer cells depend on human nucleoside transporters (hNTs) and thymidine kinase (TK). hNTs are upregulated in proliferating cells (41) and TK is also upregulated in CSCs (42). *De novo* synthesis of thymidine is catalyzed by thymidylate synthase and inhibition of the enzyme increased uptake and incorporation of iodinated thymidine analogs, also in CSCs (17,19).

[<sup>125</sup>I]I-UdR decreased the viability of all three tumorsphere samples, with LUC6 being the most sensitive and LUC10 and LUC13 the most resistant, results which were supported by the clonogenic assay. The sphere formation assay is based on the ability of CSCs to divide infinitely, whereas the viability assay is based on the metabolic capacity of the cells. However, LUC13 incorporated less [<sup>125</sup>I]I-UdR within the 7 h incorporation assay and exhibited a longer doubling time, which may be reflected in the decreased response to Auger emission compared to LUC10 and LUC6. LUC10, on the other hand, incorporated the highest amount of [<sup>125</sup>I]I-UdR and was more resistant than at least LUC6. However, based on the present results, it is not possible to conclude whether LUC13 is more resistant than LUC10 or whether the result was due to decreased incorporation.

The tumorspheres exhibited increased phospho-H2AX, G2/M phase arrest, as well as induction of apoptosis, which was expected, since the emission of Auger electrons leads to DNA double-strand breaks and cell cycle arrest through checkpoint activation, which is essential in the radiation response, as it provides cells with sufficient time to repair damaged DNA or undergo apoptosis (15,20). Although it was observed that [<sup>125</sup>I]I-UdR decreased viability in all three samples, with LUC6 being the most sensitive, there was no considerable difference in apoptosis induction among the three tumorsphere specimens. Besides apoptosis, DNA damage may also lead to mitotic catastrophe due to entering mitosis with damaged DNA and is prevailing in cells lacking functional apoptotic pathways and is frequently observed in epithelial cells (43).

It has previously been indicated that CSCs are resistant to external radiation and that external radiation increases the proportion of CSCs. This may be due to the eradication of the radiation-sensitive non-stem cancer cells or, as was indicated by previous studies, the induction of stem cell-like properties in non-CSCs (44-47). However, based on the clonogenic assay of the present study, [<sup>125</sup>I]I-UdR did not increase the CSC frequency but also targeted the CSCs, as also reported previously (17,19,21).

Limitations to the present study include that only three tumorsphere samples were analyzed. Coincidentally, the tumorspheres included in the present study were of three different histological types, which challenges a comparison between histology and response. Future work should include additional tumorspheres and more 'common' histologies, such as adenocarcinoma and planocellular carcinoma. This would allow for comparison of the different histologies concerning

CSC content and sensitivity to Auger electrons. The experiments of the present study were performed *in vitro*. The next steps should include the characterization of the tumorspheres *in vivo* regarding CSC content, expression of CSC markers, Auger electron therapy and analyses of the response. In the present study, the response after seven days was analyzed; this time-point was selected due to the relatively long half-life of [<sup>125</sup>I] (60 days). However, it may be worthwhile to analyze the response after a shorter duration to understand the early cellular response. It may also be interesting to elucidate the cell death response, e.g., the involvement of caspases or mitotic catastrophe, the latter of which was reported to be involved in the radiation response (43). Furthermore, sorting the cells into CSCs and non-CSCs prior to Auger electron therapy would allow us to analyze the response in distinct cell populations and not a mixed population as was performed in the present study. However, as described previously, identifying suitable CSC markers remains challenging (34,35).

In conclusion, patient-derived long-term lung tumorspheres enriched in CSCs were established and characterized. The frequency of cells with sphere-forming potential varied, as LUC10 and LUC13 contained a higher number than LUC6. The tumorspheres with the highest frequency of CSCs exhibited slower proliferation. The slower proliferating LUC10 and LUC13 were more resistant to the Auger-emitting thymidine analog [<sup>125</sup>I]I-UdR than LUC6.

### Acknowledgements

The authors thank Consultant Karen Ege Olsen, Department of Pathology, Odense University Hospital (Odense, Denmark) and Professor Peter Bjørn Licht, Department of Thoracic, Cardiac and Vascular Surgery, Odense University Hospital (Odense, Denmark) for recruiting the patients.

### Funding

This work was supported by grants from The Independent Research Fund Denmark, Technology and Production (grant no. 7017-00303), Director Emil C. Hertz and wife Inger Hertz' Foundation, Frode Nygaards Foundation, Simon Fougner Hartmanns family Foundation, Einar Willumsens Memorial Foundation, Odense University Hospital Research Council, Eva and Henry Fraenkels Memorial Foundation, Aase and Ejnar Danielsens Foundation, Brdr. Hartmann Foundation, Karen S. Jensens Foundation and the Hede Nielsen family Foundation.

### Availability of data and materials

The datasets used and/or analyzed in the current study are available from the corresponding author upon reasonable request.

### Authors' contributions

BBO and PFHC contributed to the conception and design of the study. KLM performed the majority of the experiments. KLM and BBO checked and confirmed the authenticity of the raw data. KLM and BBO wrote the manuscript. BBO and PFHC revised the manuscript. NL, OG, KLM, and BBO analyzed

the experimental data. All authors have read and approved the final manuscript.

### Ethics approval and consent to participate

Surgical human lung cancer samples were obtained with written informed consent. The Regional Ethics Committee of Southern Denmark approved the protocol (no. S-20140170) according to guidelines that complied with good clinical practice and the Declaration of Helsinki.

### Patient consent for publication

Not applicable.

### Competing interests

The authors declare that they have no competing interests

### References

- Sung H, Ferlay J, Siegel RL, Laversanne M, Soerjomataram I, Jemal A and Bray F: Global cancer statistics 2020: GLOBOCAN estimates of incidence and mortality worldwide for 36 cancers in 185 countries. *CA Cancer J Clin* 71: 209-249, 2021.
- Heng WS, Gosens R and Kruijff FAE: Lung cancer stem cells: Origin, features, maintenance mechanisms and therapeutic targeting. *Biochem Pharmacol* 160: 121-133, 2019.
- Chen J, Xu J, Wan T, Deng H and Li D: High-sensitive detection of small-cell lung cancer cells based on terminal deoxynucleotidyl transferase-mediated extension polymerization aptamer probe. *ACS Biomater Sci Eng* 7: 1169-1180, 2021.
- Travis WD: Pathology of lung cancer. *Clin Chest Med* 32: 669-692, 2011.
- Leonetti A, Sharma S, Minari R, Perego P, Giovannetti E and Tiseo M: Resistance mechanisms to osimertinib in EGFR-mutated non-small cell lung cancer. *Br J Cancer* 121: 725-737, 2019.
- MacDonagh L, Gray SG, Breen E, Cuffe S, Finn SP, O'Byrne KJ and Barr MP: Lung cancer stem cells: The root of resistance. *Cancer Lett* 372: 147-156, 2016.
- Prabavathy D, Swarnalatha Y and Ramadoss N: Lung cancer stem cells-origin, characteristics and therapy. *Stem Cell Investig* 5: 6, 2018.
- Wang J, Sun Z, Liu Y, Kong L, Zhou S, Tang J and Xing HR: Comparison of tumor biology of two distinct cell sub-populations in lung cancer stem cells. *Oncotarget* 8: 96852-96864, 2017.
- Singh SK, Clarke ID, Terasaki M, Bonn VE, Hawkins C, Squire J and Dirks PB: Identification of a cancer stem cell in human brain tumors. *Cancer Res* 63: 5821-5828, 2003.
- Al-Hajj M, Wicha MS, Benito-Hernandez A, Morrison SJ and Clarke MF: Prospective identification of tumorigenic breast cancer cells. *Proc Natl Acad Sci USA* 100: 3983-3988, 2003.
- O'Brien CA, Pollett A, Gallinger S and Dick JE: A human colon cancer cell capable of initiating tumour growth in immunodeficient mice. *Nature* 445: 106-110, 2007.
- Collins AT, Berry PA, Hyde C, Stower MJ and Maitland NJ: Prospective identification of tumorigenic prostate cancer stem cells. *Cancer Res* 65: 10946-10951, 2005.
- Kim CF, Jackson EL, Woolfenden AE, Lawrence S, Babar I, Vogel S, Crowley D, Bronson RT and Jacks T: Identification of bronchioalveolar stem cells in normal lung and lung cancer. *Cell* 121: 823-835, 2005.
- Raniszevska A, Kwiecień I, Rutkowska E, Rzepecki P and Domagala-Kulawik J: Lung cancer stem cells-origin, diagnostic techniques and perspective for therapies. *Cancers (Basel)* 13: 2996, 2021.
- Kassis AI: Molecular and cellular radiobiological effects of Auger emitting radionuclides. *Radiat Prot Dosimetry* 143: 241-247, 2011.
- Pirovano G, Jannetti SA, Carter LM, Sadique A, Kossatz S, Guru N, Demétrio De Souza França P, Maeda M, Zeglis BM, Lewis JS, *et al*: Targeted brain tumor radiotherapy using an Auger emitter. *Clin Cancer Res* 26: 2871-2881, 2020.

17. Morgenroth A, Vogg AT, Ermert K, Zlatopolskiy B and Mottaghy FM: Hedgehog signaling sensitizes glioma stem cells to endogenous nano-irradiation. *Oncotarget* 5: 5483-5493, 2014.
18. Chan C, Fonge H, Lam K and Reilly RM: Effectiveness and normal tissue toxicity of Auger electron (AE) radioimmunotherapy (RIT) with [<sup>111</sup>In]In-Bn-DTPA-nimotuzumab in mice with triple-negative or trastuzumab-resistant human breast cancer xenografts that overexpress EGFR. *Nucl Med Biol* 80-81: 37-44, 2020.
19. Morgenroth A, Vogg AT, Zlatopolskiy BD, Siluschek M, Oedekoven C and Mottaghy FM: Breaking the invulnerability of cancer stem cells: Two-step strategy to kill the stem-like cell subpopulation of multiple myeloma. *Mol Cancer Ther* 13: 144-153, 2014.
20. Balagurumoorthy P, Xu X, Wang K, Adelstein SJ and Kassis AI: Effect of distance between decaying (<sup>125</sup>I) and DNA on Auger-electron induced double-strand break yield. *Int J Radiat Biol* 88: 998-1008, 2012.
21. Thisgaard H, Halle B, Aaberg-Jessen C, Olsen BB, Therkelsen AS, Dam JH, Langkjær N, Munthe S, Nægren K, Høilund-Carlson PF and Kristensen BW: Highly effective Auger-electron therapy in an orthotopic glioblastoma xenograft model using convection-enhanced delivery. *Theranostics* 6: 2278-2291, 2016.
22. Herreros-Pomares A, de-Maya-Girones JD, Calabuig-Fariñas S, Lucas R, Martínez A, Pardo-Sánchez JM, Alonso S, Blasco A, Guijarro R, Martorell M, *et al*: Lung tumorspheres reveal cancer stem cell-like properties and a score with prognostic impact in resected non-small-cell lung cancer. *Cell Death Dis* 10: 660, 2019.
23. Lee J, Kotliarova S, Kotliarov Y, Li A, Su Q, Donin NM, Pastorino S, Purow BW, Christopher N, Zhang W, *et al*: Tumor stem cells derived from glioblastomas cultured in bFGF and EGF more closely mirror the phenotype and genotype of primary tumors than do serum-cultured cell lines. *Cancer Cell* 9: 391-403, 2006.
24. Xie F, Xiao P, Chen D, Xu L and Zhang B: miRDeepFinder: A miRNA analysis tool for deep sequencing of plant small RNAs. *Plant Mol Biol*: Jan 31, 2012 (Epub ahead of print).
25. Livak KJ and Schmittgen TD: Analysis of relative gene expression data using real-time quantitative PCR and the 2(-Delta Delta C(T)) method. *Methods* 25: 402-408, 2001.
26. Madsen KL, Therkelsen ASN, Langkjær N, Olsen BB and Thisgaard H: Auger electron therapy of glioblastoma using [<sup>125</sup>I]5-iodo-2'-deoxyuridine and concomitant chemotherapy-evaluation of a potential treatment strategy. *Nucl Med Biol* 96-97: 35-40, 2021.
27. Shigdar S, Lin J, Li Y, Yang CJ, Wei M, Zhus Y, Liu H and Duan W: Cancer stem cell targeting: The next generation of cancer therapy and molecular imaging. *Ther Deliv* 3: 227-244, 2012.
28. Lawrence TS, Davis MA, Maybaum J, Stetson PL and Ensminger WD: The effect of single versus double-strand substitution on halogenated pyrimidine-induced radiosensitization and DNA strand breakage in human tumor cells. *Radiat Res* 123: 192-198, 1990.
29. Dupertuis YM, Vazquez M, Mach JP, De Tribolet N, Pichard C, Slosman DO and Buchegger F: Fluorodeoxyuridine improves imaging of human glioblastoma xenografts with radiolabeled iododeoxyuridine. *Cancer Res* 61: 7971-7977, 2001.
30. Rogakou EP, Pilch DR, Orr AH, Ivanova VS and Bonner WM: DNA double-stranded breaks induce histone H2AX phosphorylation on serine 139. *J Biol Chem* 273: 5858-5868, 1998.
31. Rothkamm K, Krüger I, Thompson LH and Löbrich M: Pathways of DNA double-strand break repair during the mammalian cell cycle. *Mol Cell Biol* 23: 5706-5715, 2003.
32. Lv D, Hu Z, Lu L, Lu H and Xu X: Three-dimensional cell culture: A powerful tool in tumor research and drug discovery. *Oncol Lett* 14: 6999-7010, 2017.
33. Eramo A, Lotti F, Sette G, Pillozzi E, Biffoni M, Di Virgilio A, Conticello C, Ruco L, Peschle C and De Maria R: Identification and expansion of the tumorigenic lung cancer stem cell population. *Cell Death Differ* 15: 504-514, 2008.
34. Qiu X, Wang Z, Li Y, Miao Y, Ren Y and Luan Y: Characterization of sphere-forming cells with stem-like properties from the small cell lung cancer cell line H446. *Cancer Lett* 323: 161-170, 2012.
35. Bertolini G, Roz L, Perego P, Tortoreto M, Fontanella E, Gatti L, Pratesi G, Fabbri A, Andriani F, Tinelli S, *et al*: Highly tumorigenic lung cancer CD133+ cells display stem-like features and are spared by cisplatin treatment. *Proc Natl Acad Sci USA* 106: 16281-16286, 2009.
36. Pece S, Tosoni D, Confalonieri S, Mazzarol G, Vecchi M, Ronzoni S, Bernard L, Viale G, Pelicci PG and Di Fiore PP: Biological and molecular heterogeneity of breast cancers correlates with their cancer stem cell content. *Cell* 140: 62-73, 2010.
37. Kim SY, Lee JY, Kim DH, Joo HS, Yun MR, Jung D, Yun J, Heo SG, Ahn BC, Park CW, *et al*: Patient-derived cells to guide targeted therapy for advanced lung adenocarcinoma. *Sci Rep* 9: 19909, 2019.
38. Yeon SE, No da Y, Lee SH, Nam SW, Oh IH, Lee J and Kuh HJ: Application of concave microwells to pancreatic tumor spheroids enabling anticancer drug evaluation in a clinically relevant drug resistance model. *PLoS One* 8: e73345, 2013.
39. Roesch A, Fukunaga-Kalabis M, Schmidt EC, Zabierowski SE, Brafford PA, Vultur A, Basu D, Gimotty P, Vogt T and Herlyn M: A temporarily distinct subpopulation of slow-cycling melanoma cells is required for continuous tumor growth. *Cell* 141: 583-594, 2010.
40. Park E, Park SY, Sun PL, Jin Y, Kim JE, Jheon S, Kim K, Lee CT, Kim H and Chung JH: Prognostic significance of stem cell-related marker expression and its correlation with histologic subtypes in lung adenocarcinoma. *Oncotarget* 7: 42502-42512, 2016.
41. Plotnik DA, Emerick LE, Krohn KA, Unadkat JD and Schwartz JL: Different modes of transport for 3H-thymidine, 3H-FLT, and 3H-FMAU in proliferating and nonproliferating human tumor cells. *J Nucl Med* 51: 1464-1471, 2010.
42. Tsunekuni K, Konno M, Haraguchi N, Koseki J, Asai A, Matsuoka K, Kobunai T, Takechi T, Doki Y, Mori M and Ishii H: CD44/CD133-positive colorectal cancer stem cells are sensitive to trifluridine exposure. *Sci Rep* 9: 14861, 2019.
43. Eriksson D and Stigbrand T: Radiation-induced cell death mechanisms. *Tumour Biol* 31: 363-372, 2010.
44. Al-Assar O, Muschel RJ, Mantoni TS, McKenna WG and Brunner TB: Radiation response of cancer stem-like cells from established human cell lines after sorting for surface markers. *Int J Radiat Oncol Biol Phys* 75: 1216-1225, 2009.
45. Ghisolfi L, Keates AC, Hu X, Lee DK and Li CJ: Ionizing radiation induces stemness in cancer cells. *PLoS One* 7: e43628, 2012.
46. Lagadec C, Vlashi E, Della Donna L, Dekmezian C and Pajonk F: Radiation-induced reprogramming of breast cancer cells. *Stem Cells* 30: 833-844, 2012.
47. Wang Y, Li W, Patel SS, Cong J, Zhang N, Sabbatino F, Liu X, Qi Y, Huang P, Lee H, *et al*: Blocking the formation of radiation-induced breast cancer stem cells. *Oncotarget* 5: 3743-3755, 2014.